J. Mod. Opt. 58, 1278-1284 (2011)

doi: 10.1080/09500340.2011.604735

N-step linear phase-shifting algorithms with optimum signal to noise phase demodulation

A. González [a] [*1] M. Servin [a], J. C. Estrada [a] and H. C. Rosu [b]

[a] *Centro de Investigaciones en Óptica A. C., Loma del Bosque 115, León Gto. 37150, México;* [b] *IPICYT, Instituto Potosino de Investigacion Cientifica y Tecnologica, Camino a la Presa San José 2055, San Luis Potosi S.L.P. 78216, México*

A common way to test an optical wavefront is to use a phase-shifting interferometer along with (for example) a 3-step **linear** phase shifting algorithm (PSA). The following fundamental question arises: what phase-step should be used? Typically, $\pi/2$, $2\pi/3$, or $\pi/3$ are used and in fact, any phase-step within the open interval $(0,\pi)$ can be employed. In the absence of any measuring noise, all these phase-shifts yield the same estimate for the modulating phase. However, which of these phase-steps ω_0 is the best to obtain the least noisy phase estimation from a temporal set of 3 noisy interferograms?. In this paper, working in the frequency space, a general procedure to obtain the optimum phase-step ω_0 of a given **linear** *n*-step PSA is given. This general procedure is exemplified to some particular **linear** PSAs, notably 3, 5, 7, and 27-step PSAs.

Phase shifting algorithm; quadrature filter; signal to noise ratio

1 Introduction

Linear temporal phase-shifting algorithms (PSAs) are widely used to estimate the modulating phase of interferograms [1-5]. **Linear** PSAs incorporate a constant phase-step ω_0 (in radians/interferogram) to obtain a set of interferometric data [2-5]. It is well known that the more temporal interferograms we have, the less noisy is the phase that

[1 *] Corresponding author. Email: adonai@cio.mx

we estimate; for example a 5-step **linear** PSA will provide (in general) less noisy phase demodulation than a 3-step one [5-6]. However, if we are restricted to take, say 5 temporal interferograms, an interesting piece of information to be aware of is: which value for the phase-step ω_0 should be used in a 5-step **linear PSA** to obtain the least noisy demodulated phase? In this paper, we answer this question in a general way (not just for a 5-step **linear** PSA), and apply it to some concrete examples. A proper use of the procedure presented in this paper (necessarily) involves **linear** tunable *N*-step PSAs.

It is worth to mention that PSAs may be clasified in three large groups:

- Constat phase-step linear PSAs:

  These PSAs are phase estimating formulas in which the phase-step is constant. An example of a linear PSA with constant phase step ($\omega_0 = \pi / 2$) is the 5-step Schwider-Hariharan algorithm [8,9]:

$$\hat{\phi}(x,y) = \arctan \frac{2\left[I(-1) - I(1)\right]}{2I(0) - I(-2) - I(2)}; \quad \omega_0 = \frac{\pi}{2}. \qquad (1)$$

  Where $\hat{\phi}(x,y)$ is the estimated modulating phase.

- Variable phase-step linear (*tunable*) PSAs:

  In a tunable phase-step PSAs, the explicit appearence of the phase-step ω_0 is given. We may generate an infinite number of linear tunable PSAs by selecting a real-value ω_0 within the interval $(0,\pi)$. An example of a 5-step linear-tunable PSA is [10]:

$$\hat{\phi}(x,y)|_{t=0} = \arctan \frac{2\left[I(-1) - I(1)\right]\sin(\omega_0)}{2I(0) - I(-2) - I(2)}; \quad \omega_0 \in (0,\pi) \qquad (2)$$

- Non-linear *self-tuning* PSAs

  Non-linear self-tuning PSAs is an algorithm that do not need an explicit value of ω_0 in the PSA's arctangent ratio. The estimation of the frequency carrier ω_0 is given by an algebraic combination of the interferograms' data. That is, a formula using the intensities of the interferograms give an estimate for ω_0 [11-17]. Stoilov et. al. designed the followig 5-steps non-linear *self-tuning* PSA [8]:

$$\hat{\phi}(x,y)|_{t=0} = \arctan \frac{2\left[I(-1)-I(1)\right]\sqrt{1-\left[\dfrac{I(-2)-I(2)}{2\left[I(-1)-I(1)\right]}\right]^2}}{2I(0)-I(-2)-I(2)}. \tag{3}$$

  Comparing Eq. (3) with Eq. (2), we can see that $\sin(\omega_0)$ is given as the square root of a non-linear algebraic combination of the interferometric data.

It is easy to note that Eq. (1) is derived from Eq. (2), by setting ω_0 to π/2; the result is the Schwider-Hariharan linear (constant phase-step) PSA. In turn, Eq. (3) is an extension of Eq. (2); the term $\sin(\omega_0)$ is given by the square-root estimator.

The first impression is that **linear** tunable PSAs are hard to design, but as we show they are not difficult to construct. Once having a mathematical model for a **linear** tunable PSA (with explicit dependence on ω_0 as in Eq. (2)), we look for the best carrier ω_0 within the interval $(0,\pi)$ that maximizes the signal to noise ratio of the demodulated phase.

2 Phase shifting interferometry

The standard mathematical model for an interferogram corrupted by additive noise is:

$$I(x,y,t) = a(x,y,t) + b(x,y,t)\cos[\phi(x,y)+\omega_0 t] + n(x,y,t),\ t \in (0,1\ldots). \tag{4}$$

In this equation $a(x,y)$ is the background illumination, $b(x,y)$ is the contrast of the fringes, $\phi(x,y)$ is the phase being measured, ω_0 is the phase-step (or frequency carrier) used, and finally $n(x,y,t)$ is an additive corrupting noise. The additive noise is considered Gaussian, stationary, white, with flat-power spectral density of $S(\omega)=\eta/2$. We know that additive noise is not the only kind of interferometric measuring noise. There is also the multiplicative or phase-noise that is attributable to speckles because of the coherent laser illumination used. However, once a linear low-pass filter is applied for cleaning-up the fringe data, the multiplicative noise turns into additive Gaussian noise by the law of large numbers [7]. Moreover, after using several times a 3x3-averaging filter, one normally ends up with reasonably clear (still corrupted by some additive noise) fringes [7] as modeled in Eq. (4). The signal in Eq. (4) can be decomposed into complex components as follows:

$$I(t)=a+\frac{b}{2}\exp[i(\phi+\omega_0 t)]+\frac{b}{2}\exp[-i(\phi+\omega_0 t)]+n(t). \qquad (5)$$

The explicit dependence (x,y) of the signals has been omitted for clarity. To obtain the searched analytical signal $(b/2)\exp[i(\phi+\omega_0 t)]$ one needs to filter-out the low-frequency background $a(x,y)$, and the complex signals $(b/2)\exp[-i(\phi+\omega_0 t)]$. Assuming tha the complex term at $+\omega_0$ is kept, the **linear** PSA (a quadrature filter) must have a frequency transfer function (FTF) $H(\omega)$ with at least the following frequency response [4,5]

$$H(-\omega_0)=0 \quad H(0)=0 \quad H(\omega_0)\neq 0. \ (6)$$

Applying this FTF function $H(\omega)$ to the interferograms the following complex output signal is obtained [4,5]:

$$F^{-1}[I(\omega)H(\omega)]_{t-0} = I(t) * h(t)\big|_{t=0} = \frac{b}{2} H(\omega_0)\exp(\omega_0)\exp(i\phi) + \bar{n}\exp(i\Phi). \quad (7)$$

$F[\cdot]$ is the Fourier transform operator and $F^{-1}[\cdot]$ its inverse. The symbol * denotes the one-dimensional (over t) convolution, and $h(t)$ is the quadrature's filter impulse response associated with the PSA, with FTF $H(\omega) = F[h(t)]$ [5]. The term $\bar{n}\exp(i\Phi)$ is a complex random-variable associated to the Gaussian additive output noise. Finally, Φ is a random (phase noise) process uniformly distributed within the interval $[0, 2\pi]$ [7]. The estimated phase at $t = 0$ is given by the **linear** PSA associated to $h(t)$ as [5]:

$$\hat{\phi}(x, y) = \frac{Im[I(x, y, t) * h(t)]}{Re[I(x, y, t) * h(t)]}\bigg|_{t=0}, \qquad (8)$$

where the operators $Re[\cdot]$ and $Im[\cdot]$ take the real and the imaginary part of their argument. The hat over $\hat{\phi}(x, y)$ denotes its estimated value that may differ from the true phase $\phi(x, y)$ stated in Eq. (4).

In the next section, we describe two spectral **linear tunable** PSA models. The first analyzed spectrum is the tunable 3-step **linear** PSA, which is the simplest and probably the most frequently used algorithm. Later on, we analyze PSAs with 5, 7, 27-steps using another tunable spectral model finding the best carrier ω_0 that maximizes the *S/N* ratio. Other **linear** tunable *N*-step PSA spectral models can be easily defined, although they may have different optimal carriers ω_0.

3 Linear tunable phase shifting algorithms

As was mentioned in the introduction of this paper, to find the best ω_0 that maximizes the *S/N* we need linear tunable PSAs. In this paper we construct linear tunable PSAs by combining first-order digital filter, or by combining second-order digital linear filters. Repeated convolutions of these first or second order digital filters leads to higher order linear PSAs.

3.1 Linear tunable PSAs by combining first-order digital filter

We construct linear tunable PSAs by combining two simple first-order digital linear filters. The basic mathematical model for these first-order filters are:

$$h_1(t) = \delta(t) - \delta(t-1), \qquad (9)$$

$$h_1(t,\omega_0) = [\delta(t) - \delta(t+1)]\exp(-i\omega_0 t), \qquad (10)$$

where $\delta(t)$ is the Dirac delta function, and $i = \sqrt{-1}$. The frequency transfer function (FTF) of these basic models are:

$$F[h_1(t)] = H_1(\omega) = 1 - \exp(i\omega), \qquad (11)$$

$$F[h_1(t,\omega_0)] = H_1(\omega,\omega_0) = 1 - \exp[-i(\omega - \omega_0)], \qquad (12)$$

the combination of several first-order blocks leads to the desired *N*-step linear tunable PSA's FTF [18]. A spectral-model for high-order *N*-step linear tunable PSA may be given by:

$$H_N(\omega,\omega_0) = H_1^n(\omega)H_1^m(\omega,\omega_0)\ ;\ N = n + m + 1, \qquad (13)$$

Where the number of possible steps *N* is $3, 4, 5, 6, ..., n + m + 1$. The simplest example of this construction model is a 3-step lineat tunable PSA. This filter has the following FTF:

$$H_3(\omega,\omega_0) = H_1^1(\omega)H_1^1(\omega,\omega_0) = (1 - e^{i\omega})[1 - e^{i(\omega_0 - \omega)}] \quad (14)$$

taking the inverse fourier transform $F^{-1}[\cdot]$ of Eq. (14), $h_3(t,\omega_0)=F^{-1}[H_3(\omega,\omega_0)]$ one obtains the complex impulse response of the linear 3-step PSA tuned at ω_0.

$$h_3(t,\omega_0)=-\delta(t-1)+\delta(t)+\exp(i\omega_0)\delta(t)-\exp(i\omega_0)\delta(t+1),\ \omega_0\in(0,\pi) \qquad (15)$$

by using Eq. (8) and Eq. (15) one obtains a 3-step linear PSA tuned at ω_0 as [19]:

$$\hat{\phi}(x,y)\,|_{t=0}=\arctan\left\{\frac{\sin(\omega_0)[I(0)-I(1)]}{-I(-1)+I(0)+\cos(\omega_0)[I(0)-I(1)]}\right\};\quad \omega_0\in(0,\pi) \qquad (16)$$

The equation above represent a 3-step linear *tunable* PSA, the spectral amplitude $|H_3(\omega,\omega_0)|$ is shown in Fig. 1 for $\omega_0=2\pi/3$. The complex harmonics rejected by this linear tunable PSA are clearly identify from the plot. In this particular frequency span the complex harmonics rejected are: $(...,-6,-4,-3,-1,2,3,5,6,...)$.

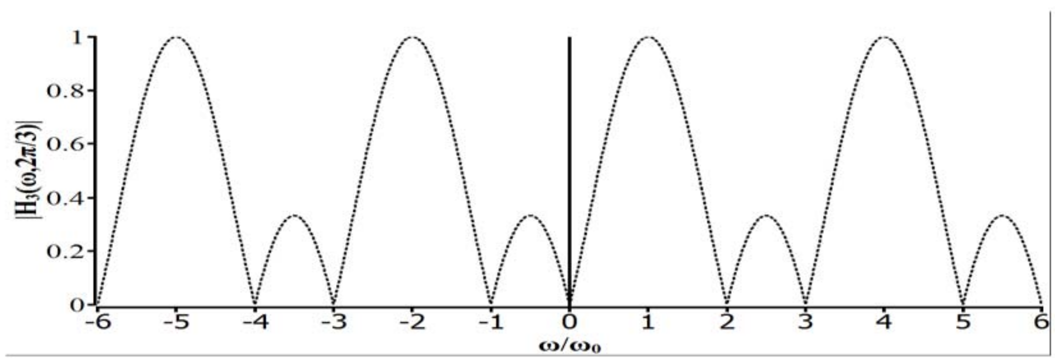

Figure 1: The 3-step linear PSA, tuned at $\omega_0=2\pi/3$. It is shown in this paper that the optimum carrier that minimizes the demodulated phase-noise of this linear PSAs is $2\pi/3$. In this particular figure the complex harmonic rejected are: $(...,-6,-4,-3,-1,2,3,5,6,...)$.

3.2 Linear tunable PSAs by combining second-order digital filters

In this sub-section we construct **linear** tunable PSAs by combining two second-order digital linear filters. Repeated convolutions of these two (second order) filters leads to higher order **linear** PSAs. In other words, several convolutions of these two simple building blocks generate arbitrary high order **linear** tunable PSAs [20]. The mathematical forms of these **second-order** filters are:

$$h_2(t) = i\,[\delta(t-1) - \delta(t+1)] \quad (17)$$

$$h_2(t,\omega_0) = -\exp(-i\omega_0)\delta(t-1) + 2\delta(t) - \exp(i\omega_0)\delta(t+1). \quad (18)$$

The frequency transfer function (FTF) of these filters are:

$$F[h_2(t)] = H_2(\omega) = -2\sin(\omega) \quad (19)$$

$$F[h_2(t,\omega_0)] = H_2(\omega,\omega_0) = 2 - 2\cos(\omega - \omega_0). \quad (20)$$

$H_2(\omega)$ filters-out the background $a(x,y)$ at $\omega = 0$, and also the components at $\omega = (\ldots,-2\pi,-\pi,0,\pi,2\pi,\ldots)$. On the other hand, the filter $H_2(\omega-\omega_0)$ can be frequency-tuned to any ω_0 (within $(0,\pi)$), removing the complex signal at $\omega = -\omega_0$ and letting pass its conjugate at $\omega = \omega_0$ (see Eq. (6)). The simplest spectral product of these two building blocks gives the FTF of a 5-step tunable PSA:

$$H_5(\omega,\omega_0) = H_2(\omega)H_2(\omega-\omega_0)\,; \quad \omega_0 \in (0,\pi) \quad (21)$$

This spectrum complies with Eq. (6), which gives the minimum conditions for a valid **linear** tunable PSA. Taking the inverse Fourier transform of Eq. (21), one obtains the complex impulse response of a 5-step **linear tunable** quadrature filter $h_5(t,\omega_0) = F^{-1}[H_5(\omega,\omega_0)]$,

$$h_5(t,\omega_0) = -i\exp(-i\omega_0)\delta(t-2) + 2i\delta(t-1) + \\ i\exp(-i\omega_0)\delta(t) - i\exp(i\omega_0)\delta(t) - 2i\delta(t+1) + i\exp(i\omega_0)\delta(t+2). \qquad (22)$$

As this equation shows, the impulse response $h_5(t,\omega_0)$ depends on the choice of the phase-step ω_0 used. Finally, according to Eq. (8), one obtains a **linear** 5-step PSA tuned at ω_0 as,

$$\hat{\phi}(x,y)\,|_{t=0} = \arctan\left\{\frac{2[I(-1)-I(+1)]+\cos(\omega_0)[I(+2)-I(-2)]}{\sin(\omega_0)[2I(0)-I(+2)-I(-2)]}\right\}. \qquad (23)$$

Note that this **linear** tunable 5-step PSA reduces to the Schwider-Hariharan **linear** PSA for $\omega_0 = \pi/2$ [8, 9]. A useful spectral-model for higher order **linear** PSAs is obtained by combining $H_2(\omega)$ and higher powers of $H_2(\omega,-\omega_0)$, increasing the detuning robustness of the PSA at ω_0. In other words higher power of $H_2(\omega,-\omega_0)$ flattens the **linear** PSAs spectral response at ω_0 [5,18]. Therefore, the spectral-model for this high-order N-step **linear** tunable PSAs considered in this paper has the form:

$$H_N(\omega,\omega_0) = H_2(\omega)[H_2(\omega-\omega_0)]^{\frac{N-5}{2}+1},\ N = 5, 7, 9, 11, \ldots \qquad (24)$$

For example, one can obtain the spectrum of a N = 27-step PSA tuned at $\omega_0 = \pi/2$ as,

$$H_{27}(\omega,\pi/2) = H_2(\omega)[H_2(\omega-\pi/2)]^{12}. \qquad (25)$$

Figure 2 shows the spectra of a 5-step, 7-step, and 27-step **linear** PSAs all tuned at $\omega_0 = \pi/2$, obtained by Eq. (24). The left side complex signal at $\omega = -\pi/2$ is zero for all 5, 7 and 27-step **linear** PSAs, while being transparent at $\omega = \pi/2$. The 27-step **linear** PSA spectrum is (almost) flat-zero for $\omega \in (-\pi, 0)$ as a consequence it has very small detuning error [5, 18]. In these particular cases the complex harmonics rejected are: $(\ldots,-8,-6,-5,-4,-2,-1,2,3,4,6,7,8,\ldots)$. Also as Fig. 2 shows, these quadrature filters are very robust to detuning at these harmonics. Finally, the **linear** tunable PSA that results from this *N*-step spectral model Eq. (24) applied to our set of *N* phase-shifted interferograms $I_N(x,y,t)$ is:

$$\hat{\phi}(x,y)=\arctan\left\{\left.\frac{Im[h_N(t,\omega_0)*I_N(x,y,t)]}{Re[h_N(t,\omega_0)*I_N(x,y,t)]}\right|_{t=0}\right\};\quad \omega_0\in(0,\pi) \qquad (26)$$

where $h_N(t,\omega_0)=F^{-1}[H_N(\omega,\omega_0)]$.

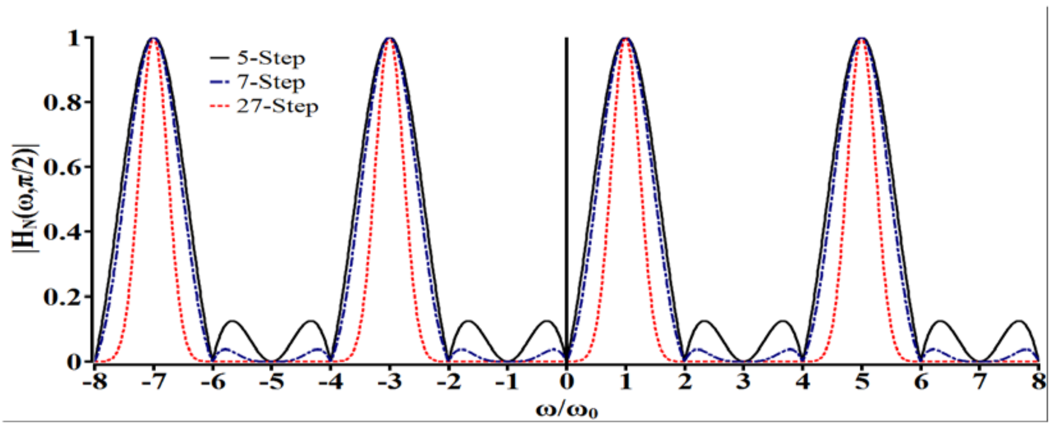

Figure 2: Linear tunable PSAs with 5, 7 and 27-steps with spectral model given by Eq. (24). These quadrature filters remove the DC term at $\omega=0$ and the complex frequency component at $\omega=-\pi/2$. The complex harmonics rejected are: $(\ldots,-8,-6,-5,-4,-2,-1,2,3,4,6,7,8,\ldots)$. These harmonics rejections are robust to detuning.

4 Optimum phase-step to obtain the maximum *S/N* ratio gain

This section describes the objective of this paper, namely obtain the optimal carrier ω_0^{opt} for **linear tunable** PSAs to obtain the best signal to noise (*S/N*) power ratio. As far as we know, the optimal value ω_0^{opt} for a given linear PSA's spectral model that renders the least noisy demodulated phase has not been published.

We assume that the output-power noise $\overline{n}$ in Eq. (7) is substantially less than the amplitude of the output complex signal, i.e. $\overline{n} << H(-\omega_0,\omega_0)b/2$; additive low-noise approximation. This condition is normally fulfilled when the interferograms are low-pass filtered to remove some noise [5,6]. Under these circumstances, the *S/N* power-ratio of the output phase can be demonstrated to be [6]

$$\left[\frac{S}{N}(\omega_0)\right]_{output} = \frac{\left|H(\omega_0)\right|^2}{\frac{1}{2\pi}\int_{-\pi}^{\pi} H(\omega,\omega_0)H^*(\omega,\omega_0)d\omega}\left[\frac{S}{N}\right]_{input} = G(\omega_0)\left[\frac{S}{N}\right]_{input} . \quad (27)$$

Where $(S/N)_{\text{input}}$ is the interferogram's signal to noise power ratio. $H(\omega,\omega_0)$ stands for the filter's spectrum (which depends on the interferogram's carrier ω_0), and $H^*(\omega,\omega_0)$ stands for its complex conjugate. $G(\omega_0)$ is the algorithm's (*S/N*) power gain. Note that the *S/N* algorithm's gain $G(\omega_0)$ is a function of the carrier frequency ω_0 alone. In other words, given a mathematical spectral model for **linear tunable** PSAs, $H(\omega,\omega_0)$ we may choose the carrier ω_0 which maximizes this power-ratio gain $G(\omega_0)$ in Eq. (27).

4.1 Optimum ω_0 to obtain the best (S/N) ratio for a 3-step linear PSA

Owing to its wide use, let us first analyze the spectrum of a 3-step **linear** tunable PSA and find the optimum carrier that minimizes its demodulated phase noise. The 3-step **linear** PSA tuned at ω_0, has the following formula [15,19]:

$$\hat{\phi}(x,y) = \arctan\left\{\frac{[1-\cos(\omega_0)][I(x,y,-1)-I(x,y,1)]}{\sin(\omega_0)[2I(x,y,0)-I(x,y,-1)-I(x,y,1)]}\right\}; \quad \omega_0 \in (0,\pi) \quad (28)$$

The temporal impulse response associated with this **linear** tunable PSA is [4, 5]

$$h_3(t,\omega_0)=\sin(\omega_0)[2\delta(0)-\delta(t+1)-\delta(t-1)]+i\{[1-\cos(\omega_0)][\delta(t-1)-\delta(t+1)]\} \quad (29)$$

and its FTF (in this case real) $H(\omega,\omega_0)$ is:

$$H_3(\omega,\omega_0)=F[h_3(t,\omega_0)]=2\sin(\omega_0)[1-\cos(\omega)]-2[1-\cos(\omega_0)]\sin(\omega);\ \omega_0\in(0,\pi) \quad (30)$$

Finally, using Eq. (27) one obtains the S/N ratio gain $G(\omega_0)$ for a 3-step algorithm as follows:

$$G(\omega_0)_{\hat{\phi}}=\frac{|H_3(\omega_0)|^2}{\frac{1}{2\pi}\int_{-\pi}^{\pi}|H_3(\omega,\omega_0)|^2\,d\omega};\quad \omega_0\in(0,\pi) \qquad (31)$$

This last equation states the importance of having a **linear** tunable PSA in order to find the best tuning frequency ω_0 within the interval $(0,\pi)$. Equation (31) shows that the *S/N* ratio gain $G(.)$ depends only on ω_0; therefore setting the derivative of this equation (with respect to ω_0) equal to zero one obtains the optimum ω_0^{opt} which renders the *S/N* power ration gain $G(\omega_0)$ maximum. In the case of the 3-step **linear** PSA, the optimum phase-shift is:

$$\frac{d\,G(\omega_0)}{d\omega_0}\Big|_{\omega_0^{opt}=2\pi/3}=0. \qquad (32)$$

This correspond to the optimal carrier frequency $\omega_0^{opt}=2\pi/3$

Figure 1 shows the FTF, $H_3(\omega,2\pi/3)$, corresponding to the optimum-carrier 3-step **linear** PSA. This **linear** PSA filters out the complex signal at $\omega=-2\pi/3$, while the complex signal at $\omega=2\pi/3$ is allowed to pass. With this result one is now absolutely certain that a carrier of $2\pi/3$ is the best choice to obtain the cleanest demodulated phase for a 3-step **linear** PSA corrupted by additive noise. **Table 1 shows**

the FTF for the 3, 5, 7, and 27-step linear tunable PSA models used in this paper.

Table 2 shows the PSAs for the 3, 5, and 7-step FTFs in table 1.

Table 1: *N*-step linear PSA construction results

N-step	Filter Spectral Response (FTF)
3	$H_3(\omega,\omega_0)=\sin(\omega_0)-\sin(\omega_0-\omega)-\sin(\omega)$
5	$H_5(\omega,\omega_0)=\sin(\omega_0)-\sin(\omega_0-2\omega)-2\sin(\omega)$
7	$H_7(\omega,\omega_0)=\sin(\omega_0)+\sin(2\omega_0-3\omega)-\sin(\omega-2\omega)-\sin(2\omega_0-\omega)-\sin(\omega)$
27	$H_{27}(\omega,\omega_0)=\sin(\frac{\omega_0-\omega}{2})^{24}\sin(\omega)$

Table 2: Linear tunable PSA

N step	Linear tunable PSA
3	$\hat{\phi}_3(\omega,\omega_0)=\arctan\left(\frac{I(-1)-I(1)+\cos(\omega_0)(I(1)-I(-1))}{\sin(\omega_0)(I(-1)+2I(0)-I(1))}\right);\omega_0\in(0,\pi)$
5	$\hat{\phi}_5(\omega,\omega_0)=\arctan\left(\frac{-\cos(\omega_0)(I(-2)+I(2))+I(-1)-I(1)}{\sin(\omega_0)(I(-2)+I(0)-I(2))}\right);\omega_0\in(0,\pi)$
7	$\hat{\phi}_7(\omega,\omega_0)=$ $\arctan\left(\frac{\cos(2\omega_0)(I(-3)+I(3)-I(-1)+I(1))+\cos(\omega_0)(I(2)-I(-2))+3(I(-1)-I(1))}{\sin(2\omega_0)(I(-3)+I(3)-I(1)-I(-1))+\sin(\omega_0)(2I(0)-I(2)-I(-2))}\right);\omega_0\in(0,\pi)$

4.2 Optimum phase-step to obtain the maximum S/N gain in higher order linear tunable PSAs

The main purpose of this sub-section is to calculate the optimum temporal carrier ω_0^{opt} from Eq. (27). Using these second-order filters we obtain the spectra for the 5, 7, and 27-step spectra in Table 1. The optimum carrier ω_0^{opt} is the one that gives the lowest noise in the phase demodulation process for the **linear *N*-step** PSA's spectral model in Eq. (24). Figure. 3 shows four graphs corresponding to the $G(\omega_0)$ ratio gain of 3, 5, 7, and 27-step **linear** tunable PSAs. The $G(\omega_0)$ power-ratio gain depends solely on the carrier frequency ω_0 (see Eq. (27)). Higher order **linear** PSAs, modeled by Eq. (24), $H_N(\omega,\omega_0)=H_2(\omega)H_2(\omega,\omega_0)^{(N-5)/2+1}$, all have their maximum signal to noise gain $G(.)$ at $\omega_0^{opt}=\pi/2$

$$G(\pi/2)_{Maximum}=\frac{\left|H_N(\pi/2)\right|^2}{\frac{1}{2\pi}\int_{-\pi}^{\pi}\left|H_N(\omega,\pi/2)\right|^2 d\omega};\quad \omega_0=\frac{\pi}{2} \qquad (33)$$

The step-angle of $\pi/2$ is a frequently chosen value in experimental work. Figure 3 also shows the intuitive result that, the more steps we have, the higher (optimum) *S/N* ratio is obtained. From Eq. (23), we see that for $N=5$-steps, and $\omega_0=\pi/2$ we obtain the Schwider-Hariharan PSA. Therefore, the Hariharan-Schwider **linear** PSA uses the best possible carrier within its spectral model in Eq. (24).

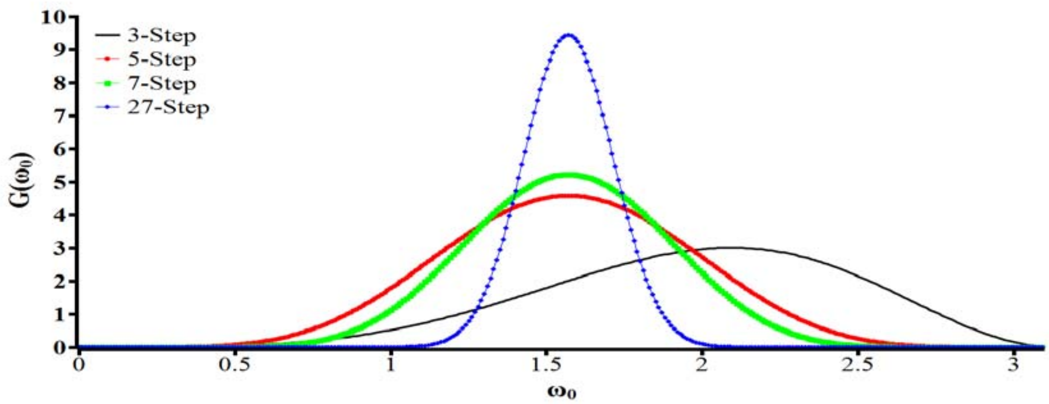

Figure 3: This figure shows the best frequency carrier through the *S/N* analysis performed herein as the main objective of this paper.

5 Conclusions

This paper shows a technique to find the optimum phase-shift ω_0^{opt} which maximizes the signal to noise ratio (*S/N*) on the demodulated phase for **linear** tunable PSAs. This holds true whenever the corrupting interferogram noise is additive, white, and Gaussian. To apply our procedure, one needs a **linear** tunable PSA' spectral model to vary ω_0 and keep the one that maximizes the $G(\omega_0)$ ratio in Eq. (27). The particular spectral models used in this paper were presented in Eq. (13) and Eq. (24). These two spectral models were substituted into Eq. (27), and the best carrier ω_0 that maximizes *S/N* ratio gain, $G(\omega_0)$ is chosen. This optimization was applied to 3, 5, 7, and 27-step **linear** tunable PSAs. We have found that for the case of a 3-step **linear** PSA, the carrier that maximizes the $G(\omega_0)$ ratio is $\omega_0^{opt} = 2\pi/3$, while for the spectral model in Eq. (24), the best $G(\omega_0)$ ratio gain is obtained by $\omega_0^{opt} = \pi/2$. This optimizing procedure can be easily extended to other **linear** tunable PSA spectral models not considered here. Note the important fact that, the optimum value for ω_0 depends on the PSA' spectral model chosen. For example, one may have two 5-step **linear tunable** PSAs with different spectral model, having possibly two different optimum carriers that optimize $G(\omega_0)$.

References

[1] K. Freischlad and C. L. Koliopoulos. Fourier description of digital phase-measuring interferometry. *J. Opt. Soc. Am. A*, 7(4):542-551, 1990.

[2] D. W. Phillion. General methods for generating phase--shifting interferometry algorithms. *Appl. Opt.*, 36(31):8098-8115, 1997.

[3] Yves Surrel. Design of algorithms for phase measurements by the use of phase stepping. *Appl. Opt.*, 35(1):51-60, 1996.

[4] Daniel Malacara and Brian J. Thompson M. *Handbook of Optical Engineering* of TECHNOLOGY & ENGINEERING Optics. Marcel Dekker Inc, 1 edition, 2001.

[5] M. Servin and J. C. Estrada and J. A. Quiroga. The general theory of phase shifting algorithms. *Opt. Express*, 17(24):21867-21881, 2009.

[6] Yves Surrel. Additive noise effect in digital phase detection. *Appl. Opt.*, 36(1):271-276, 1997.

[7] M. Servin and J. C. Estrada and J. A. Quiroga and J. F. Mosino and M. Cywiak. Noise in phase shifting interferometry. *Opt. Express*, 17(11):8789-8794, 2009.

[8] J. Schwider and R. Burow and K. E. Elssner and J. Grzanna and R. Spolaczyk and K. Merkel. Digital wave-front measuring interferometry: some systematic error sources. *Appl. Opt.*, 22(21):3421-3421, 1983.

[9] P. Hariharan and B. F. Oreb and T. Eiju. Digital phase-shifting interferometry: a simple error-compensating phase calculation algorithm. *Appl. Opt.*, 26(13):2504-2506, 1987.

[10] G. Stoilov and T. Dragostinov. Phase-stepping interferometry: five-frame algorithm with an arbitrary step. *Opt. Las. Eng.*, 28:61-69, 1997.

[11] P. Carré. Installation et utilisation du comparateur photoelectrique et interferentiel du bureau international des poids et measures. *Metrologia*, 2(1):13-23, 1966.

[12] Kieran G. Larkin. Efficient nonlinear algorithm for envelop detection in white light interferometry. *J. Opt. Soc. Am. A*, 13(4):832-843, 1996.

[13] Jiri Novak. Five-step phase-shifting algorithms with unknown values of phase shift. *Optik*, 114:63-68, 2003.

[14] Quian Kemao and Shu Fangjun and Wu Xiaoping. Determination of the best phase step of the Carré algorithm in phase shifting interferometry. *Meas. Sci. Technol.*, 11:1220-1223, 2000.

[15] M. Servin and F. J. Cuevas. A novel technique for spatial phase-shifting interferometry. *Journal of Modern Optics*, 42:1853-1862, 1995.

[16] Julio C. Estrada and Manuel Servin and Juan A. Quiroga. A self-tuning phase-shifting algorithm for interferometry. *Opt. Express*, 18(3):2632-2638, 2010.

[17] J. A. Gomez-Pedro and J. A. Quiroga and M. Servin. Temporal evaluation of fringe patterns with spatial carrier with an improved asynchronous phase demodulation algorithm. *Journal of Modern Optics*, 10:97-109, 2004.

[18] A. Gonzalez and M. Servin and J. C. Estrada and J. A. Quiroga. Design of Phase Shifting Algorithms by fine-tuning spectral-shaping. *Opt. Express*, 19:10692-10697, 2011.

[19] Daniel Malacara. *Optical shop testing*. Wiley & Sons, third edition, 2007.

[20] J. C. Estrada and M. Servin and J. A. Quiroga. Easy and straightforward construction of wideband phase-shifting algorithms for interferometry. *Opt. Lett.*, 34(4):413-415, 2009.